Doping the nematic liquid crystal 5CB with milled BaTiO_{3} nanoparticles

Alexander Lorenz, Natalie Zimmermann, Satyendra Kumar, Dean R. Evans, Gary Cook, and Heinz-S. Kitzerow

Phys. Rev. E **86**, 051704 — Published 20 November 2012

DOI: 10.1103/PhysRevE.86.051704

Doping the Nematic Liquid Crystal 5CB with Milled $BaTiO_3$ Nanoparticles

Alexander Lorenz[1], Natalie Zimmermann[1], Satyendra Kumar[2], Dean R. Evans[3], Gary Cook[3,4], and Heinz-S. Kitzerow[1]

[1]Department of Chemistry, University of Paderborn, Warburger Str. 100, 33098 Paderborn, Germany
[2]Department of Physics, Kent State University, Kent, Ohio 44242, USA
[3]Air Force Research Laboratory, Materials and Manufacturing Directorate, Wright-Patterson Air Force Base, Ohio 45433, USA
[4]Azimuth Corporation, 4134 Linden Avenue, Suite 300, Dayton, Ohio 45432, USA

The simple nematic mesogen 5CB was doped with milled $BaTiO_3$ nanoparticles and investigated with x-ray scattering. Doping with $BaTiO_3$ nanoparticles of 9 nm in diameter led to the formation of crystallites. These crystallites precipitated and formed a wax-like nano-dispersion of 5CB and nanoparticles which led to intense x-ray scattering signals characteristic for a multilayer structure. Surprisingly, the multilayers possess unusual interlayer spacing which cannot be explained by simple smectic order of the calamitic molecules.

I. INTRODUCTION

Doping of nematic liquid crystals (LCs) with a small mass fraction of inorganic nanoparticles is of great scientific interest. For example, silica nanoparticles and silica nanoparticles carrying covalently bond surface functionalization were investigated [1,2]. Recently, the impact of nanoscale particles has been highlighted [3]. For example, a small dopant concentration of surface functionalized nanoparticles can improve the electro-optical performance of LCs or cause induced dual alignment effects [3,4]. Nanoparticles surface functionalized with proto-mesogenic ligands may even self-assemble into nanoparticulate thermotropic liquid-crystalline materials [5,6]. Another approach to surface functionalize nanoparticles is to use surfactants like oleic acid. This method is in particular useful to dope LCs with ferroelectric nanoparticles, e.g. $BaTiO_3$ nanoparticles. For example, ferroelectric nanoparticles coated with a surfactant and dispersed in nematic LCs were reported to enhance the optical diffraction efficiency of beam coupling [7,8], alter the dielectric anisotropy, shift the phase transition temperatures [9,11], and cause asymmetry in the electro-optic response of LCs [11]. Recently, it was reported that dispersions of $BaTiO_3$ nanoparticles can be prepared by milling cubic $BaTiO_3$ in heptane with oleic acid in a planetary ball mill [12]. Nanoparticles of 9 nm in average diameter suspended in heptane were obtained by milling for 25 h [12,13]. Stressed $BaTiO_3$ nanoparticles, which possess permanent electric polarization, can be extracted from such dispersions by harvesting [14].

This work is focused on x-ray investigations of possible changes in the liquid crystal structure of a simple nematic mesogen caused by doping with inorganic $BaTiO_3$ nanoparticles. In the present experiments, the well-known nematic LC 4-cyano-4'-pentylbiphenyl (5CB) was doped

with milled $BaTiO_3$ nanoparticles. The LC 5CB shows a nematic phase at ambient temperature and has a clearing temperature of 37 °C. The 5CB molecule has a length of 1.8 nm and forms dimers with a length of 2.5 nm in the isotropic and nematic phase [15,16]. The dimerization is strong in the bulk and may be decrease by surface effects due to polar interactions [17]. The crystalline phase of 5CB also contains dimers [18]. These dimers are stabilized by dipole-dipole interactions between the cyano-biphenyl groups. In the crystal lattice, the 5CB molecules form a layered structure where each molecular layer possesses one adjacent layer of antiparallel and parallel oriented molecules, respectively. The interlayer distance of two antiparallel oriented layers is only slightly smaller than the interlayer distance between two parallel oriented layers. Thus, the crystal is also characterized by strong London interactions between parallel oriented 5CB molecules. The nanoparticles used for doping were fabricated by milling [12, 13] and the resulting heptane dispersion of nanoparticles (9 nm in average diameter) was used for doping without further purification. The doped LC was investigated with both small angle x-ray scattering (SAXS) and wide angle x-ray scattering (WAXS). The x-ray scattering signals caused by nanoparticles and by 5CB molecules were detected simultaneously. The investigation reveals that milled $BaTiO_3$ nanoparticles may cause growth of crystallites with a multilayered structure of 5CB molecules and lead to the precipitation into an amorphous material, which can be easily extracted from the LC.

II. EXPERIMENTAL PROCEDURE

A. Preparation of the nanoparticle-dispersions and doping

The $BaTiO_3$ nanoparticles were dispersed in 5CB. First, a dispersion of $BaTiO_3$ nanoparticles of 9 nm in average diameter was prepared by milling cubic (non-ferroelectric) $BaTiO_3$ for 25 h in a planetary ball mill in the presence of oleic acid as surfactant and heptane as solvent [12]. Milling resulted a dispersion of $BaTiO_3$-nanoparticles with a concentration of 45 mg/g. It is likely that the stress experienced by cubic $BaTiO_3$ particles during the milling process converted some of them into tetragonal $BaTiO_3$. Consequently, such nanoparticles in the initial dispersion will show ferroelectric properties (i.e., possess a permanent electric polarization). The initial dispersion of the milled nanoparticles was used without further purification. A doped LC sample was prepared with a concentration of c_{doping} = 5 mg/g by dissolving 0.028 g of the initial nanoparticle-dispersion in 0.25 g of pure 5CB in an open glass vessel and mixing it with a magnetic stirrer. The glass vessel along with stirrer was placed in a fume hood and the solvent was allowed to slowly evaporate at ≈ 50 °C and ambient pressure until the sample mass became constant. The mixture was continuously stirred and filled in 1.5 mm diameter quartz Lindemann capillaries. Subsequently, the capillaries were sealed with epoxy and kept vertically until the phase separation was visually observed.

B. Small and wide angle X-ray scattering

The neat LCs and the nanoparticle dispersion were investigated by x-ray diffraction at National Synchrotron Light Source (NSLS), beamline X6B. The samples were placed inside a modified Instec (HCS402) hot stage with a temperature precision of ± 0.1 °C and an *in-situ* ≈ 2.5 kG magnetic field produced by a pair of CoSm magnets. The capillaries were centered in

the x-ray beam and the temperature was adjusted to 28 °C. A Princeton Instruments CCD camera system (PI-SCX:4300/1-165) with 2084 x 2084 pixels (24 micron pixel, 50 mm chip) and 2.4:1 fiber ration option (120 x 120 mm field of view) was used as detector. For the first series of experiments, the scattering behavior in the (WAXS) region q = 1.5 to 16 nm^{-1} was studied with x-ray photon energy of 12 keV and a sample-to-detector-distance of 26 cm. Subsequently, the detector was moved to a distance of 120 cm and the scattering behavior in the region q = 0.3 to 3 nm^{-1} was investigated. Finally, x-ray photon energy was adjusted to 8 keV and the scattering was studied in the (SAXS) region q = 0.1 to 1.5 nm^{-1}. Each setup was calibrated with silver behenate [19] and the 2D diffraction patterns were analyzed with MATLAB.

III. RESULTS

A. Experiments at a constant temperature of 28 °C

The neat and doped samples were studied at a temperature of 28 °C where the neat 5CB shows a typical diffraction pattern of oriented nematic LCs [Fig. 1 (a)]. Nematic LCs show two diffuse peaks in the wide angle region (only one of them is shown). The position of these peaks corresponds to the average intermolecular separation in the direction perpendicular to the molecular long axis ($d_{\perp}$) [20]. Additionally, two narrower peaks appear in the small angle region. The position of the narrow small angle peaks corresponds to the average intermolecular separation in the direction parallel to the molecular long axis ($d_{||}$) [20]. This characteristic spacing corresponds to the length of the 5CB dimers (2.5 nm) in the nematic phase of 5CB [15]. In contrast to neat 5CB, the doped sample showed segregation into a phase separated white substance at the bottom of the capillaries. Both, the segregated substance and the more transparent, upper region, were studied separately. No significant difference between the scattering from the upper region of the sample and from the neat sample could be discerned. In contrast, x-ray diffraction patterns of the white region of the doped LC [Fig. 1 (b)] differ considerably from diffraction patterns of the neat LC [Fig. 1 (a)]. Diffraction rings appear in the diffraction patterns of the doped LC because the sample was not oriented by the magnetic field. An intense, circular peak appeared in the center of these diffraction patterns [Fig. 1 (b)]. Scattering in the wide-angle region also gave rise to a ring in the diffraction patterns rather than an oriented peak. Juxtaposition of the diffraction patterns of the neat and the doped LC [Fig. 1 (c)] shows that the wide-angle reflections in both samples are at approximately the same angle [Fig. 1 (c)]. The central peak in the diffraction patterns of the doped LC is surrounded by a ring. This ring and the small angle scattering caused by the neat compound appear at the same scattering angle. In addition to the scattering patterns recorded at 12 keV, patterns were also recorded at 8 keV, as shown in Fig. 1 (d), in the small-angle region for the doped LC.

The dependence of scattering intensity on diffraction angle (or, |scattering vector|; e.g., see Fig. 2) was extracted from two-dimensional scattering data. As already revealed by the scattering patterns, the scattering curve of the neat LC shows three peaks at approximately 2.5 nm^{-1}, 5.0 nm^{-1}, and 14.9 nm^{-1}. The peak at ≈ 5 nm^{-1} is a second order reflection of the peak at ≈ 2.5 nm^{-1}. This peak correspond to a d-spacing of $d_{||} = 2 \cdot \pi / 2.5\ nm^{-1} = 2.5$ nm, the length of a 5CB dimer, as expected [15]. The peak observed at 14.8 nm^{-1} corresponds to a spacing of

$d_{\perp}$ = 0.43 nm, which was also reported in the literature [15]. In addition to these three peaks, some scattering is also observed in the region q = 0.25 – 1.5 nm^{-1}. Presumably, this small angle scattering is caused by long range orientational order fluctuations in the neat LC. In the wide-angle region, the scattering curves of neat and doped LC both show a broad peak at q = 14.8 nm^{-1}.

In contrast to the scattering curve of the neat LC, the scattering curve of the doped LC shows strong scattering in the range q = 0.25 to ≈ 1.5 nm^{-1} caused by the dopant. In the range q > 1.4 nm^{-1}, a Bragg signal at q ≈ 1.4 nm^{-1} and 4 higher orders of this reflection centered at q ≈ 2.8, 4.2, 5.6, and 7.0 nm^{-1} can be identified in the scattering curve of the doped LC. These signals are apparently caused by a soft, multilayered structure with a characteristic spacing of d_l ≈ 4.49 nm. X-ray scattering of multilayered structures can be analyzed by means of the paracrystalline theory [reviewed in Ref. 21] under the assumption that the radius of curvature of the multilayers is large compared to the thickness of the individual layers:

$$I_{(q)} = \frac{S(q)|F(q)|^2}{q^2}. \qquad (1)$$

In this model (Eq. 1), the factor q^{-2} is the Lorentz correction for a non-oriented powder sample. The structure factor $S(q)$ describes Bragg scattering due to the crystalline nature of the layered system. The factor $F(q)$ is the form factor of the individual layers. In the paracrystalline theory, the form factor of a flat particle [22] is applied to describe the intensity variation of the Bragg peaks. The form factor of a flat particle (a layer) corresponds to the Fourier transform of the electron density distribution $\eta(r)$ parallel to the layer normal:

$$F(q) = \int_{-d/2}^{d/2} \eta(r)\cos(qr)\, dr. \qquad (2)$$

The form factor for multilayered structures describes a characteristic decay of intensity of the higher order Bragg peaks I_h proportional to q^{-2} [22]. Accordingly, in soft, multilayered structures the scattering intensity of the Bragg peaks I_h decays proportional to the peak intensity of the fundamental peak:

$$I_h = I_1 / q^4. \qquad (3)$$

The scattering curve of the doped LC was modeled with 5 Lorentzians centered at the positions q = 1.4, 2.8, 4.2, 5.6, and 7.0 nm^{-1}. Three Lorentzians centered at the peak positions of the neat LC (2.5 nm^{-1}, 5 nm^{-1}, and 14.8 nm^{-1}) were also added. The two peaks at 2.5 nm^{-1} and 5 nm^{-1} account for neat LC, which is also present in the doped sample. The third peak at 14.8 nm^{-1} describes the Bragg reflection caused by $d_{\perp}$. Three different models are shown along with the experimental scattering curve of the doped LC (Fig. 2). These models differ in the decay of the amplitudes of the 5 Lorentzians centered at the positions q = 1.4, 2.8, 4.2, 5.6, and 7.0 nm^{-1}, which account for the Bragg scattering caused by the multilayer structure. The third model curve where the amplitudes of these 5 Lorentzians decay proportional to q^{-4} fits the data much better than the two model curves where the amplitudes decay proportional to q^{-2} and q^{-3}, respectively. Such a characteristic decay proportional to q^{-4} indicates a multilayered structure. Compared to the neat LC, the scattering intensity in the doped sample is higher in the range q < 2.5 nm^{-1} (Fig. 4, inset) due to scattering caused by the inorganic nanoparticles and due to the intense fundamental Bragg peak of the multilayer structure

centered at q = 1.4 nm^{-1}. According to the peak positions, the layer thickness of the individual layers corresponds to $d_l \approx 4.49$ nm. Lorentzian peaks with a full width at half maximum (FWHM) = 0.25 nm^{-1} were used in the model curves for the 5 Lorentzians centered at q = 1.4, 2.8, 4.2, 5.6, and 7.0 nm^{-1}. A FWHM of 0.25 nm^{-1} corresponds to a correlation length of $2 \cdot \pi$ / 0.25 nm^{-1} ≈ 25 nm or a minimum thickness of 5-6 layers. In the fabrication step, oleic acid was added as surfactant and oleic acid was grafted onto the nanoparticles during the milling process. The characteristic molecular spacing of a single oleic acid molecule in the crystal is 2.03 nm [23] where oleic acid shows dimerization with a characteristic spacing of not more than 4.06 nm. Both, the length of a single oleic acid molecule and the length of oleic acid dimers would not fit to the observed layer spacing. Oleic acid is not covalently bond to the nanoparticles. In the heptane dispersion, oleic acid is adsorbed at the surface of the inorganic nanoparticles. The 5CB molecules possess a polar head group, may adsorb at the surface of the $BaTiO_3$ nanoparticles and replace oleic acid molecules. Single oleic acid molecules as well as dimers may be solvated by 5CB. In the doped sample, 5CB is available even in excess concentration. Most likely, 5CB molecules replace oleic acid at the nanoparticle surface. The present results indicate that 5CB dimers form a bilayer structure. A similar phenomenon, where one to two crystalline layers were found to be present on a solid substrate in the SmA, nematic, and isotropic phases, was previously reported [24] for a simple calamitic mesogen. The thin crystalline layers were found to melt around 30 °C above the clearing point of this mesogen. In the nematic phase, 5CB molecules are well known to form dimers with a length of $l_d \approx 2.5$ nm, which is smaller than the interlayer spacing of $d_l \approx 4.49$ nm. In the crystal, 5CB molecules show both, dipole-dipole interactions and London interactions. The unusual interlayer spacing of the soft, multilayered structure may be explained by a model, where two smectic layers of 5CB dimers (each stabilized by dipole-dipole interactions) possess additional stabilization by London interactions (Fig. 3). If so, the interlayer spacing d_l would be smaller than $2 \cdot l_d$ = 5 nm, as observed in the experiment ($d_l \approx 4.49$ nm < $2 \cdot l_d$). In order to proof the structure of the multilayers, a fit of the form factor of the layered structure with a model of the electron density distribution parallel to the layer normal $\eta(r)$ would be desirable. However, in the present experiments, the remainder of neat LC in the doped LC prevents this type of analysis. In future studies of similar systems, the experimental procedure could be adjusted in order to further purify the doped LC and prevent for remainders of neat LC. Anyway, the present results show that the impact of milled $BaTiO_3$ nanoparticles on a simple calamitic mesogen like 5CB is highly non-trivial and leads to unusual molecular arrangements at the nanoparticle surface, which can contribute to the unusual behavior of nanoparticle doped LC dispersions.

B. Experiments varying temperature

Small angle x-ray scattering with a sample/detector distance of 120 cm and photon energy of 12 keV was conducted with doped 5CB. The low angle limit of the present investigations was 0.1 nm^{-1}. The scattering curves of the doped sample showed a characteristic shoulder at 1.42 nm^{-1} (Fig. 4), presumably caused by a Bragg-reflection of the multilayered structure described in III A. The scattering curve of neat 5CB at 27 °C is shown for comparison. The samples were heated above 27 °C. The scattering intensity decreased with rising temperature.

But, the shoulder at 1.42 nm^{-1} was preserved which indicates a surprising high temperature stability of the multilayered structure. The multilayers were still present at 100 °C, where heating was stopped. In the region $q < 1.4\ nm^{-1}$, the dopant caused significant scattering. The scattering in this region was studied with sample/detector distance of 120 cm and photon energy of 8 keV. Guinier-plots [22] are shown in the q-range 0.17 to 0.25 nm^{-1} (Fig. 5). With rising temperature, the curves shift to lower intensity with a characteristic step between 35 and 40 °C, where pure 5CB possesses N→I phase transition. Presumably, this step was caused by pure 5CB remaining in the solution. The slope of straight lines fitted to the data is approximately temperature independent ($s \approx 8.15\ nm^2$). The slope of Guinier plots yields a radius of gyration $R_g = (3 \cdot s)^{0.5} = 4.95$ nm [22]. Although x-ray scattering in the region $0.1\ nm^{-1} < q < 1.4\ nm^{-1}$ was dominated by the dissolved inorganic nanoparticles, the form factor could not be extracted from the scattering curves because x-ray scattering from the LC makes an additional contribution to x-ray scattering.

IV. CONCLUSIONS

In the present experiments, the liquid crystal 5CB was doped with a dispersion of milled $BaTiO_3$-nanoparticles. Growth of crystallites with a soft, multilayer structure of 5CB molecules was observed. The multilayers possessed a coherence length of ≈25 nm at ambient temperature. A wax like substance phase separated and segregated out of 5CB, which led to a large Bragg scattering with a decay of peak intensity proportional to q^{-4}, which is characteristic for soft, multilayered structures. The scattering was observed at a temperature of 100 °C, which is more than 60 °C higher than the clearing temperature of neat 5CB. It was not possible to quantitatively analyze the scattering curve and extract the form factor of the multilayer structure in order to analyze the electron density distribution parallel to the layer normal. Anyway, a qualitative model of the scattering curve based upon Lorentzian peaks was presented and the layer spacing of $d_l = 4.49$ nm was extracted from the peak positions. The unusually high layer spacing was discussed and a bilayer model was proposed where a bilayer of 5CB dimers (stabilized by dipole-dipole-interactions) is stabilized by non-polar interactions and grafted onto the surface of the nanoparticles. The multilayer showed high temperature stability similar to a phenomenon reported in the literature for bilayers of another simple calamitic mesogen [24], which was deposited at a macroscopic solid surface. Further investigation is required in order to understand the tendency of multilayer formation with interlayer distance that cannot be explained by smectic order of low symmetry. The results show an unusual assembly of a simple calamitic mesogen in a complex structure. The surface functionalized nanoparticles could easily be extracted and may be used as dopants for different LCs. In such systems, it will be interesting to see if the molecules of new LC undergo exchange with the adsorbed molecules as has been reported [25] in a different system for the surface of LC-test cells. For future experiments, it will be essential to further purify the samples. If so, a quantitative analysis of the scattering curve will be possible. It would be interesting to investigate different homologues of *n*CB in order to test the influence of chain length and odd-eve effects on the interlayer spacing of the presently reported multilayers

ACKNOWLEDGEMENTS

The authors would like to thank Vesna Stanic and Elaine DiMasi (NSLS, Brookhaven National Laboratory) for their technical support and help in these experiments. Financial support by the German Research Foundation (KI 411/14 and GRK 1464), the European Science Foundation (EUROCORES, SONS II, "Self-organized nanostructures") is gratefully acknowledged. Participation of SK in this research was supported by the US Department of Energy, Office of Science, Basic Energy Sciences grant DE-SC0001412. Use of the National Synchrotron Light Source, Brookhaven National Laboratory, was supported by the U.S. Department of Energy, Office of Science, Office of Basic Energy Sciences, under Contract No. DE-AC02-98CH10886.

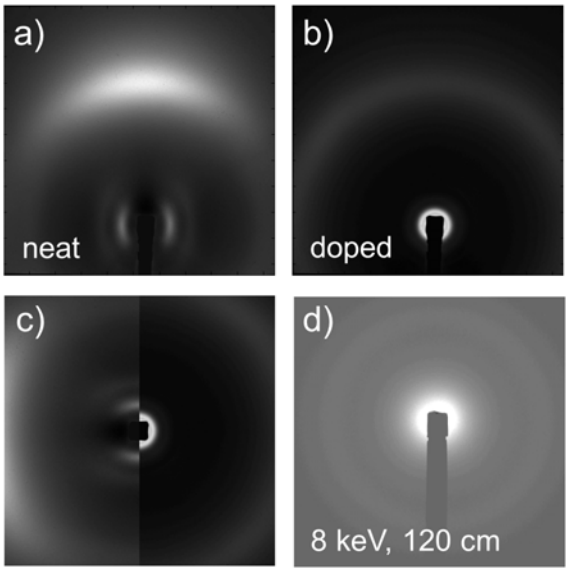

FIG. 1. Two-dimensional x-ray diffraction patterns of neat 5CB (a) and nanoparticle-doped 5CB (b, d) recorded at a temperature of 28 °C. (a, b) WAXS-patterns recorded at 12 keV photon energy and 26 cm sample/detector distance. (c) Juxtaposition of (a) and (b). (d) SAXS-pattern of doped 5CB.

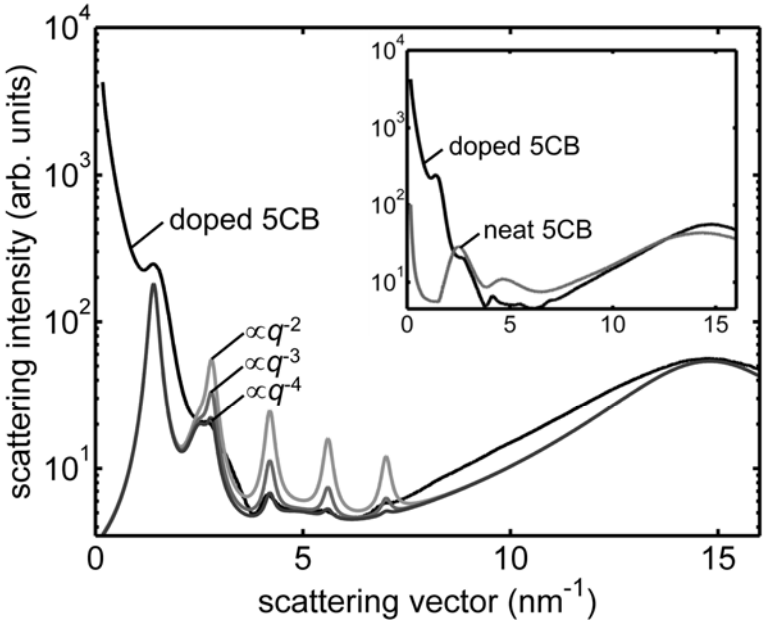

FIG. 2. Experimentally recorded scattering curve of nanoparticle-doped 5CB and three model curves with Bragg peak amplitudes proportional to q^{-2}, q^{-3} and q^{-4}, respectively. The inset shows the scattering curves of nanoparticle-doped and neat 5CB in comparison. The shown scattering curves were recorded at a temperature of 28 °C. The data was acquired with x-ray photon energy of 8 and 12 keV and sample/detector distance of 120 (SAXS-region) and 26 cm (WAXS-region), respectively. The two sets of data were then merged by matching at q = 1.5 nm^{-1}.

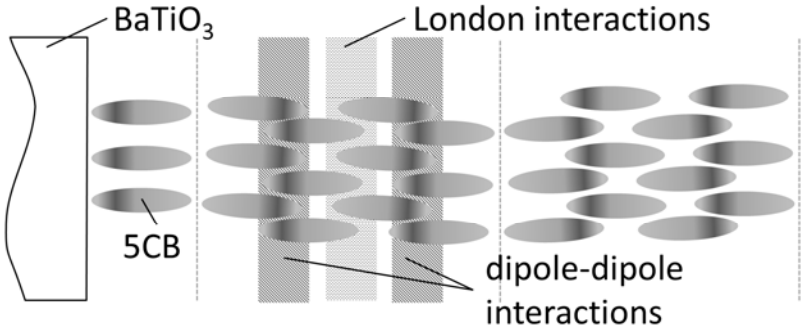

FIG. 3. Scheme of a multilayer of 5CB molecules with high interlayer distance grafted onto the surface of a $BaTiO_3$ nanoparticle. The individual layers are stabilized by dipole-dipole interactions and London interactions.

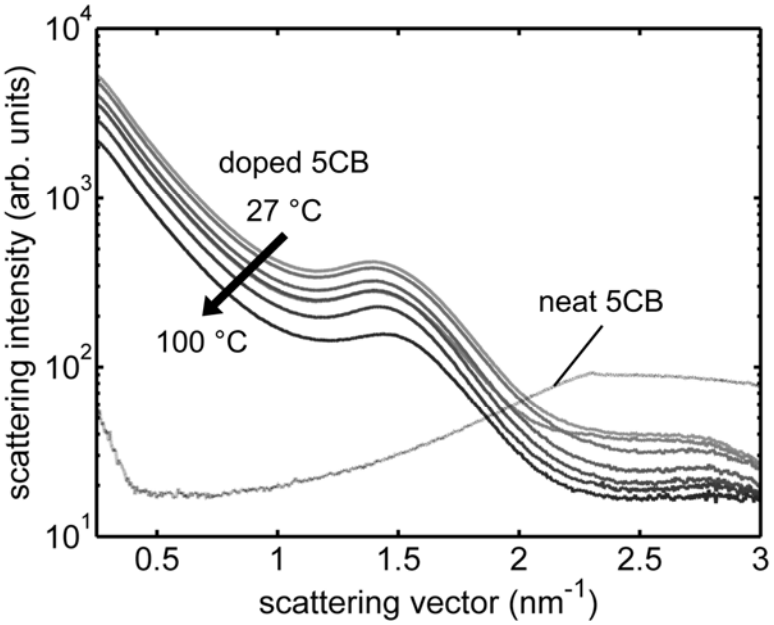

FIG. 4. Scattering curves of doped 5CB (at 27, 35, 40, 55, 70, 85, 100 °C) and neat 5CB (at 27 °C) recorded with a 12 keV x-ray beam and sample/detector distance of 120 cm.

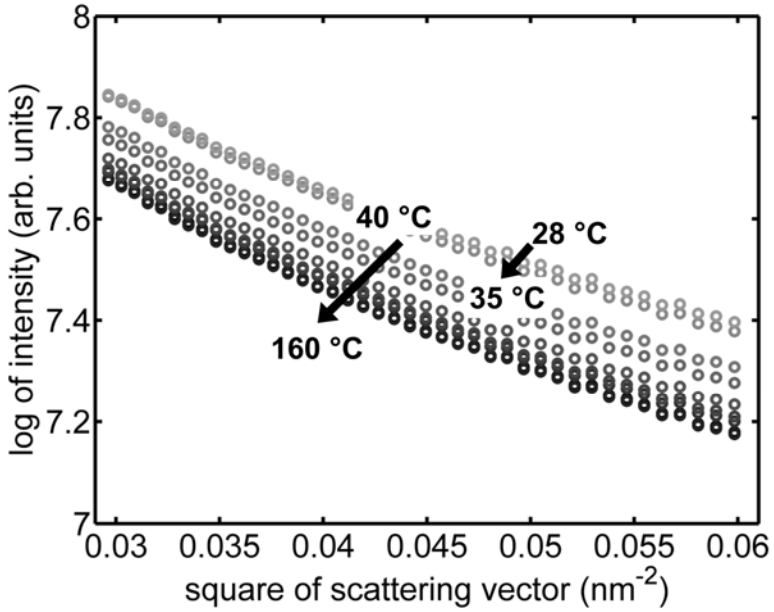

FIG. 5. Guinier plots of small-angle x-ray scattering data recorded for nanoparticle doped 5CB at temperatures of 28, 35, 40, 60, 80, 100, 120, and 160 °C.

References

1. M. Kreuzer, T. Tschudi, R. Eidenschink, Mol. Cryst. Liq. Cryst. **223**, 219 (1992).
2. A. V. Glushchenko, G. Ya. Guba, N. Yu. Lopukhovich, V. M. Ogenko, V. Yu. Reshetnyak, Yu. A. Reznikov, O. V. Yaroshchuk, Mol. Cryst. Liq. Cryst. **262**, 111 (1995).
3. H. Qui, T. Hegmann, J. Mater. Chem. **18**, 3288 (2008).
4. M. Urbanski, B. Kinkead,T. Hegmann, H.-S. Kitzerow, Liquid Crystals **37**, 1151 (2010).
5. G. L. Nealon, R. Greget, C. Dominguez, Z. T. Nagy, D. Guillon, J.-L. Gallani, B. Donnio, Beilstein J. Org. Chem. **8**, 349 (2012).
6. M. Wojcik, W. Lewandowski, J. Matraszek, J. Mieczkowski, J. Borysiuk, D. Pociecha, E. Gorecka, Angew. Chem. Int. Ed. **48**, 5167 (2009).
7. O. Buchnev, A. Dyadyusha, M. Kaczmarek, V. Reshetnyak, and Y. Reznikov, J. Opt. Soc. Am. B **24**, 1512 (2007).
8. G. Cook, A. V. Glushchenko, V. Reshetnyak, A. T. Griffith, M. A. Saleh, and D. R. Evans, Opt. Express **16**, 4015–4022 (2008).
9. A. Glushchenko, C. I. Cheon, J. West, F. Lic, E. Büyüktanir, Y. Reznikovd, A. Buchnev, Mol. Cryst. Liq. Cryst. **453**, 227-237 (2006).
10. F. Li, O. Buchnev, C. I. Cheon, A. Glushchenko,V. Reshetnyak,Y. Reznikov,T. J. Sluckin, J. L. West, Phys. Rev. Lett. **97**, 147801 (2006).
11. G. Cook, V. Yu. Reshetnyak, R. F. Ziolo, S. A. Basun, P. P. Banerjee, D. R. Evans, Opt. Express **18**, 17339 (2010).
12. H. Atkuri, G. Cook, D. R. Evans, C.-I. Cheon, A. Glushchenko, V. Reshetnyak, Y. Reznikov, J. West, and K. Zhang, J. Opt. A: Pure Appl. Opt. **11**, 024006 (2009).
13. S. A. Basun, G. Cook, V. Yu. Reshetnyak, A. V. Glushchenko, and D. R. Evans, Phys. Rev. B **84**, 024105 (2011).
14. G. Cook, J. L. Barnes, S. A. Basun, D. R. Evans, R. F. Ziolo, A. Ponce, V. Yu. Reshetnyak, A. Glushchenko, P. P. Banerjee, J. Appl. Phys. **108**, 064309 (2010).
15. A. J. Leadbetter, A. I. Mehtam, Mol. Cryst. Liq. Cryst. (Letters) **72**, 51 (1981),
16. F. Vandenbrouck, S. Bardon, M. P. Valignat, A. M. Cazabat, Phys. Rev. Lett. **81**, 610 (1998).
17. T. Sakai, K. Shirota, T. Yamada, H. Hoshi, K. Ishikawa, H. Takezoe and A. Fukuda Jpn. J. Appl. Phys. **35**, 3971 (1996).
18. T. Hanemann, W.Haase, I. Svoboda, H. Fuess, Liquid Crystals **19**, 699 (1995).
19. T. C. Huang, H. Toraya, T. N. Blanton, Y. Wu, J. Appl. Cryst. **26**, 180 (1993).
20. S. Kumar, *Liquid Crystals* (Cambridge University Press, UK, 2001).
21. J. Lemmich, K. Mortensen, J. H. Ipsen, T. Hønger, R. Bauer, O. G. Mouritsen, Phys. Rev. E **53**, 5169 (1996).
22. O. Glatter, O. Kratky, *Small Angle X-ray Scattering* (Academic Press, London, 1982).
23. S. Abrahamsson, I. Ryderstedt-Nahringbauer, Acta Cryst. **15**, 1261 (1962).
24. Y. Shi, B. Cull, S. Kumar, Phys. Rev. Lett. **71**, 2773 (1993).
25. R. Guo, Y. Reznikov, K. Slyusarenko, S. Kumar, Appl. Phys. Lett. **92**, 121911 (2008).